

β -Ga₂O₃ Nano-membrane Negative Capacitance Field-effect Transistor with Steep Subthreshold Slope for Wide Bandgap Logic Applications

Mengwei Si, Lingming Yang, Hong Zhou, and Peide D. Ye*

School of Electrical and Computer Engineering and Birck Nanotechnology Center, Purdue University, West Lafayette, Indiana 47907, United States

* Address correspondence to: yep@purdue.edu (P.D.Y.)

ABSTRACT

Steep-slope β -Ga₂O₃ nano-membrane negative capacitance field-effect transistors (NC-FETs) are demonstrated with ferroelectric hafnium zirconium oxide in gate dielectric stack. Subthreshold slope less than 60 mV/dec at room temperature is obtained for both forward and reverse gate voltage sweeps with a minimum value of 34.3 mV/dec at reverse gate voltage sweep and 53.1 mV/dec at forward gate voltage sweep at $V_{DS}=0.5$ V. Enhancement-mode operation with threshold voltage ~ 0.4 V is achieved by tuning the thickness of β -Ga₂O₃ membrane. Low hysteresis of less than 0.1 V is obtained. The steep-slope, low hysteresis and enhancement-mode β -Ga₂O₃ NC-FETs are promising as nFET candidate for future wide bandgap CMOS logic applications.

KEYWORDS: β -Ga₂O₃, wide bandgap, steep-slope, hafnium zirconium oxide, ferroelectric, negative capacitance

MAIN TEXT

▪ INTRODUCTION

High temperature solid-state devices and circuits are required for many applications such as aerospace, automotive, nuclear instrumentations and geothermal wells^{1,2}. Silicon based complementary metal-oxide-semiconductor (CMOS) technology are not able to operate at such high temperatures, which is limited by its relatively small bandgap of 1.12 eV. CMOS circuits using wide bandgap semiconductors are promising in these high temperature logic applications. Monoclinic β -Ga₂O₃ is one of the promising candidates as n-type channel material because of its ultra-wide bandgap of 4.6-4.9 eV and high electron mobility of $\sim 100 \text{ cm}^2/\text{V}\cdot\text{s}$ ³⁻¹⁰. The ultra-wide bandgap can suppress the carrier distribution at the tail of Boltzmann distribution at high temperature. Meanwhile, β -Ga₂O₃ also has the advantage to have low-cost native bulk substrates that can be synthesized in large size through melt-grown Czochralski, edge defined film fed growth, and floating zone method¹¹⁻¹⁶. To reduce the power consumption in wide bandgap CMOS logic circuits, enhancement-mode operation with threshold voltage (V_T) greater than zero and small subthreshold slope (SS) are required, similarly to Si CMOS. Because enhancement-mode operation and small SS reduce both static leakage current and the supply voltage¹⁷. SS of metal-oxide-semiconductor field-effect transistors (MOSFETs) is limited by the Boltzmann thermal distribution of electrons as $2.3 k_B T/q$, which is around 60 mV/dec at room temperature. SS would increase much more for conventional MOSFETs operated at high temperatures. Negative capacitance FETs (NC-FETs) have been proposed and attracted much attention to overcome this thermionic limit of SS¹⁸. In an NC-FET, an insulating ferroelectric material layer is inserted in the gate stack and serves as a negative capacitor so that channel surface potential can be amplified

more than the gate voltage, and hence the device can operate with SS less than 60 mV/dec at room temperature. Hafnium zirconium oxide (HZO) is a recently discovered CMOS compatible ferroelectric thin film insulator with the ability to maintain ferroelectricity with ultrathin physical thickness down to less than 2 nm¹⁹⁻²³. Therefore, the integration of wide bandgap semiconductors and ferroelectric HZO can reduce the thermionic SS degradation at high temperatures and useful to reduce power consumption in high temperature logic applications.

In this paper, we demonstrate β -Ga₂O₃ NC-FETs with ferroelectric hafnium zirconium oxide in gate dielectric stack. Subthreshold slope less than 60 mV/dec at room temperature is obtained for both forward and reverse gate voltage (V_{GS}) sweeps with a minimum value of 34.3 mV/dec at reverse gate voltage sweep and 53.1 mV/dec at forward gate voltage sweep at $V_{DS}=0.5$ V. Enhancement-mode operation is achieved by tuning the thickness of β -Ga₂O₃ with V_T of 0.47 V for forward gate voltage sweep, V_T of 0.38 V for reverse gate voltage sweep and a low hysteresis less than 0.1 V.

▪ EXPERIMENTS

Fig. 1(a) shows the schematic diagram of β -Ga₂O₃ NC-FETs, which consists of 86 nm thick β -Ga₂O₃ nano-membrane as the channel, 3 nm amorphous aluminum oxide (Al₂O₃) layer and 20 nm polycrystalline HZO layer as the gate dielectric, heavily n-doped (n⁺⁺) silicon substrate as the gate electrode and Ti/Au source/drain as the metal contacts. The silicon substrate was firstly cleaned by RCA standard cleaning and diluted HF dip, to remove organic, metallic contaminants, particles and unintentional oxides, followed deionized water rinse and drying. The substrate was then transferred to an atomic layer deposition (ALD) chamber to deposit 20 nm Hf_{1-x}Zr_xO₂ film at 250 °C, using [(CH₃)₂N]₄Hf (TDMAHf), [(CH₃)₂N]₄Zr (TDMAZr), and H₂O as the Hf precursor,

Zr precursor, and oxygen precursor, respectively. The $\text{Hf}_{1-x}\text{Zr}_x\text{O}_2$ film with $x = 0.5$ was achieved by controlling $\text{HfO}_2:\text{ZrO}_2$ cycle ratio to be 1:1. To encapsulate the $\text{Hf}_{1-x}\text{Zr}_x\text{O}_2$ film, 3 nm Al_2O_3 was subsequently *in-situ* deposited by using $\text{Al}(\text{CH}_3)_3$ (TMA) and H_2O as precursors at the same 250 °C, to prevent the degradation of HZO by the reaction with moisture in air. The amorphous Al_2O_3 layer is also used for capacitance matching and gate leakage current reduction. The importance of this interfacial Al_2O_3 layer on capacitance matching is discussed in detail in Ref. 23. A rapid thermal annealing (RTA) in nitrogen ambient was then performed for 1 minute at 500 °C to enhance the ferroelectricity²³. Thin $\beta\text{-Ga}_2\text{O}_3$ nano-membrane was mechanically exfoliated and transferred to the $\text{Al}_2\text{O}_3/\text{HZO}/\text{n}^{++}$ Si substrate from a (-201) $\beta\text{-Ga}_2\text{O}_3$ bulk substrate with Sn doping concentration of $2.7 \times 10^{18} \text{ cm}^{-3}$ (Determined by C-V measurement⁷). Source and drain regions were defined by electron-beam lithography using ZEP520A as e-beam resist. Ar plasma bombardment for 30 s was then applied to generate oxygen vacancies to enhance the surface n-type doping for the reduction of the contact resistance, followed by Ti/Au (30/60 nm) electron-beam evaporation and lift-off processes. Fig. 1(b) shows the false-color scanning electron microscope (SEM) image of the fabricated $\beta\text{-Ga}_2\text{O}_3$ NC-FETs with 4 different channel lengths on the same membrane, capturing the $\beta\text{-Ga}_2\text{O}_3$ membrane and the Ti/Au electrodes. Fig. 1(c) shows the cross-sectional TEM image of the $\text{HZO}/\text{Al}_2\text{O}_3$ gate stack. All device electrical characterizations were carried out at room temperature with a Keysight B1500 Semiconductor Parameter Analyzer and a Cascade Summit probe station.

▪ RESULTS AND DISCUSSION

Fig. 2(a) shows the polarization versus voltage hysteresis loop (P-V) for TiN/20 nm HZO/TiN capacitor at different annealing temperatures. The P-V shows clear dielectric to ferroelectric

transition of HZO after annealing, while the P-V shows weak dependence on annealing temperature above 400 °C. The metal-insulator-metal (MIM) capacitors are used for Landau coefficients (α , β , γ) extraction for ferroelectric HZO layer only. Fig. 2(b) shows the polarization versus voltage (P-V) characteristics for n++ Si/20 nm HZO/3 nm Al₂O₃/Ni stack (the same gate stack of the β -Ga₂O₃ NC-FETs) annealed at 450 °C at different voltage sweep ranges. The P-V shows clear ferroelectric hysteresis loop. The P-V characteristics of a thin film ferroelectric insulator can be modeled using Landau-Khalatnikov (L-K) equation¹⁸. The L-K equation for P-V can be expressed as $V_f = 2\alpha t_f P + 4\beta t_f P^3 + 6\gamma t_f P^5 + \rho t_f \frac{dP}{dt}$, where V_f is the voltage across the ferroelectric insulator, P is the polarization charge, t_f is the thickness of the ferroelectric insulator, $\alpha/\beta/\gamma$ are the Landau coefficients and ρ is an equivalent damping constant of the ferroelectric insulator. Landau coefficients are extracted directly from the P-V characteristics in Fig. 2(a) on ferroelectric HZO after annealing²³. The Landau coefficients are extracted by fitting to experimental data using L-K equation (assuming $dP/dt=0$ for static P-V measurement) to be $\alpha=-1.911 \times 10^8$ m/F, $\beta=4.32 \times 10^9$ m⁵/F/coul², and $\gamma=0$ m⁹/F/coul⁴, as shown in Fig. 2(c). Note that the P-V calculated from L-K equation shows S-shape where the negative dP/dV is the negative capacitance, as shown in Fig. 2(c). However, this negative dP/dV cannot be observed from experimental P-V (Fig. 2(a) and Fig. 2(b)) because of the negative capacitance state is unstable, which leads to the hysteresis in real experimental P-V measurement. Energy (U) versus charge (Q) is plotted based on experimental Landau coefficients and calculation using L-K equations as in Fig. 2(d). The negative second order derivative (d^2U/dQ^2) also indicates the existence of negative capacitance. The energy of ferroelectric capacitor tends to stay at the local minimums of the U-Q so that the negative capacitance (where $d^2U/dQ^2<0$) is unstable. As a result, NC-FETs may exhibit large hysteresis if the unstable negative capacitance effect is too strong. The key design for the β -

Ga₂O₃ NC-FETs in this work is to stabilize the unstable negative capacitance by matching the capacitance of Al₂O₃ layer (C_{ox}) and the depletion capacitance (C_D) in β -Ga₂O₃ layer with the capacitance of the ferroelectric HZO layer (C_{FE}). Therefore, low hysteresis and sub-60 mV/dec subthreshold slope at room temperature can be achieved at the same time.

Fig. 3(a) shows the normalized I_D - V_{GS} characteristics in log scale of a β -Ga₂O₃ NC-FET. The back-gate bias is swept from -0.4 V to 2 V in 40 mV per step while the drain voltage (V_{DS}) is biased at 0.1 V, 0.5 V and 0.9 V. The whole sweep takes roughly 1 minute. This device has a channel length (L_{ch}) of 0.5 μ m and channel thickness (T_{ch}) of 86 nm, measured by atomic force microscopy (AFM). This particular thickness is chosen to tune the V_T slightly above zero. If the channel is too thick, V_T is negative so that the device becomes depletion-mode while if the channel is too thin, the conducting current is very small¹⁰. The typical range of physical width of these nano-membrane devices is 0.3~1 μ m, determined by scanning electron microscopy (SEM) for the normalization of drain current. The I_D - V_{GS} characteristics were measured in bi-direction both forwardly (V_{GS} from low to high) and reversely (V_{GS} from high to low). SS is extracted as a function of I_D for both forward sweep ($SS_{min,For}$) and reverse sweep ($SS_{min,Rev}$) at various V_{DS} . Fig. 3(b)-(d) show the SS- I_D characteristics extracted from Fig. 3(a) at $V_{DS}=0.1$ V, 0.5 V and 0.9 V, respectively. The device exhibits $SS_{min,For}=57.2$ mV/dec, $SS_{min,Rev}=41.0$ mV/dec at $V_{DS}=0.1$ V, $SS_{min,For}=53.1$ mV/dec, $SS_{min,Rev}=34.3$ mV/dec at $V_{DS}=0.5$ V, and $SS_{min,For}=55.0$ mV/dec, $SS_{min,Rev}=34.4$ mV/dec at $V_{DS}=0.9$ V. SS below 60 mV/dec at room temperature is demonstrated for both forward and reverse gate voltage sweeps even at relatively high V_{DS} . Ga₂O₃ MOSFETs with 15 nm Al₂O₃ as gate dielectric exhibit minimum SS=118.8 mV/dec, as shown in supplementary section 1. SS- I_D characteristics at different V_{DS} are similar; slightly better at high V_{DS} due to the larger impact of Schottky barrier at lower V_{DS} . Because of the large bandgap of β -Ga₂O₃, the band-to-band

tunneling current at high V_{DS} is suppressed.

Fig. 4(a) shows the I_D - V_{GS} characteristics in linear scale of the same β - Ga_2O_3 NC-FET as in Fig. 3. V_T is extracted by linear extrapolation at $V_{DS}=0.1$ V for both forward and reverse gate voltage sweeps. V_T in forward gate voltage sweep ($V_{T,For}$) is extracted to be 0.47 V while V_T in reverse gate voltage sweep ($V_{T,Rev}$) is 0.38 V. Hence, enhancement-mode operation with V_T greater than zero for both forward and reverse gate voltage sweeps is demonstrated. A negligible hysteresis is obtained for both on-state (high V_{GS} , as shown in Fig. 4(a)) and off-state (low V_{GS} , as shown in Fig. 3(a)), except that when V_{GS} is near the threshold voltage region. At the threshold voltage, low hysteresis is achieved to be 90 mV, calculated by using $|V_{T,Rev}-V_{T,For}|$. Note that this hysteresis is negative if we don't take the absolute value because of the gate voltage induced polarization charge inside the ferroelectric HZO. This is in stark contrast to the conventional hysteresis from MOSFETs with interface and oxide traps, where hysteresis is usually positive because of charge trapping in the defect states. The hysteresis of NC-FETs generally comes from two origins. The one is from the unstable negative capacitance state in ferroelectric insulator ($d^2U_{FE}/dQ^2 < 0$). This hysteresis can be completely removed by well-matched capacitances (C_{FE} , C_{ox} and C_D) so that $d^2(U_{FE}+U_{ox}+U_D)/dQ^2$ is greater than zero for all Q for total capacitance to remove the unstable negative capacitance state. The stability condition (static non-hysteretic condition) for the 20 nm HZO/3 nm Al_2O_3 has been confirmed to be fulfilled in Ref. 23 so that it is not the origin of the hysteresis in the β - Ga_2O_3 NC-FETs in this work. The second origin of the hysteresis is a dynamic effect of measurement because of the ferroelectric dumping factor (ρ) in dynamic L-K equations²⁴, which can explain the hysteresis measured in the β - Ga_2O_3 NC-FETs in this work. Fig. 4(b) shows the I_D - V_{DS} characteristics of the same β - Ga_2O_3 NC-FET with V_{GS} from -0.5 V to 2.5 V in 0.5 V step and V_{DS} swept from 0 V to 2 V. A linear current-voltage relationship at low V_{DS} shows a

relatively good contact property at metal/ β -Ga₂O₃ interface. The relative low drain current in this work, compared to Ref. 10, is not clear. The interface situation of β -Ga₂O₃ on HZO gate stack seems very different from that on SiO₂ in Ref. 10. The requirement of thick β -Ga₂O₃ membrane (60 nm ~ 80 nm) to observe β -Ga₂O₃ enhancement-mode operation indicates the significant interface traps and surface depletion exhibit. Although the exact mechanism why the interface traps do *not* affect steep-slope observation on β -Ga₂O₃ NC-FETs is not clear at this moment, we suspect that it is related to the ultra-wide bandgap of β -Ga₂O₃.

▪ CONCLUSION

Steep-slope β -Ga₂O₃ negative capacitance field-effect transistors are demonstrated with ferroelectric HZO in gate dielectric stack. SS less than 60 mV/dec at room temperature is obtained for both forward and reverse gate voltage sweeps with a minimum value of 34.3 mV/dec at reverse gate voltage sweep and 53.1 mV/dec at forward gate voltage sweep at $V_{DS}=0.5$ V. Enhancement-mode operation with threshold voltage ~ 0.4 V is achieved by tuning the thickness of β -Ga₂O₃ membrane. And a low hysteresis less than 0.1 V is obtained. The steep-slope, low hysteresis and enhancement-mode β -Ga₂O₃ NC-FETs are promising nFET candidate for future wide bandgap CMOS logic applications.

ASSOCIATED CONTENT

Supporting Information.

The supporting information is available free of charge on the ACS Publication website.

Additional details of Ga₂O₃ MOSFETs with Al₂O₃ only as gate dielectric are in the supporting information.

AUTHOR INFORMATION

▪ **Corresponding Author**

*E-mail: yep@purdue.edu

▪ **Author Contributions**

P.D.Y. conceived the idea and supervised the experiments. M.S. did the ALD of HZO and Al₂O₃. H.Z. exfoliated the β-Ga₂O₃ membrane. M.S. and L.Y. did the P-V measurement. M.S. performed the device fabrication, electrical characterization and analyzed the experimental data. M.S. and P.D.Y. co-wrote the manuscript and all authors commented on it.

▪ **Funding Sources**

This material is based upon work supported by the AFOSR under Grant FA9550-12-1-0180 and in part by DTRA under Grant HDTRA1-12-1-0025.

▪ **Notes**

The authors declare no competing financial interest.

ACKNOWLEDGEMENTS

The authors would like to thank M. Fan and H. Wang for the technical support and Chun-Jung Su, S. Salahuddin, and K. Ng for valuable discussions.

REFERENCES

- (1) Casady, J. B.; Johnson, R. W. *Solid. State. Electron.* **1996**, *39*, 1409–1422.
- (2) Neudeck, P. G.; Okojie, R. S.; Chen, L.-Y. *Proc. IEEE* **2002**, *90*, 1065–1076.
- (3) Higashiwaki, M.; Sasaki, K.; Kuramata, A.; Masui, T.; Yamakoshi, S. *Appl. Phys. Lett.* **2012**, *100*, 013504.
- (4) Sasaki, K.; Kuramata, A.; Masui, T.; Villora, E. G.; Shimamura, K.; Yamakoshi, S. *Appl. Phys. Exp.* **2012**, *5*, 035502.
- (5) Higashiwaki, M.; Sasaki, K.; Kamimura, T.; Wong, M. H.; Krishnamurthy, D.; Kuramata, A.; Masui, T.; Yamakoshi, S. *Appl. Phys. Lett.* **2013**, *103*, 123511.
- (6) Hwang, W. S.; Verma, A.; Peelaers, H.; Protasenko, V.; Rouvimov, S.; Xing, H.; Seabaugh, A.; Haensch, W.; Van De Walle, C.; Galazka, Z.; Albrecht, M.; Fornari, R.; Jena, D. *Appl. Phys. Lett.* **2014**, *104*, 203111.
- (7) Zhou, H.; Alghmadi, S.; Si, M.; Qiu, G.; Ye, P. D. *IEEE Electron Device Lett.* **2016**, *37*, 1411–1414.
- (8) Wong, M. H.; Sasaki, K.; Kuramata, A.; Yamakoshi, S.; Higashiwaki, M. *IEEE Electron Device Lett.* **2016**, *37*, 212–215.
- (9) Ahn, S.; Ren, F.; Kim, J.; Oh, S.; Kim, J.; Mastro, M. A.; Pearton, S. J. *Appl. Phys. Lett.*

- 2016**, *109*, 062102.
- (10) Zhou, H.; Si, M.; Alghmadi, S.; Qiu, G.; Ye, P. D. *IEEE Electron Device Lett.* **2017**, *38*, 103–106.
- (11) Irmischer, K.; Galazka, Z.; Pietsch, M.; Uecker, R.; Fornari, R. *J. Appl. Phys.* **2011**, *110*, 063720.
- (12) Galazka, Z.; Irmischer, K.; Uecker, R.; Bertram, R.; Pietsch, M.; Kwasniewski, A.; Naumann, M.; Schulz, T.; Schewski, R.; Klimm, D.; Bickermann, M. *J. Cryst. Growth* **2014**, *404*, 184-191.
- (13) Aida, H.; Nishigushi, K.; Takeda, H.; Aota, N.; Sunakawa, K.; Yaguchi, Y. *Jpn. J. Appl. Phys.* **2008**, *47*, 8506– 8509.
- (14) Kuramata, A.; Koshi, K.; Watanabe, S.; Yamaoka, Y.; Masui, T.; Yamakoshi, S. *Jpn. J. Appl. Phys.* **2016**, *55*, 1202A2.
- (15) Ueda, N.; Hosono, H.; Waseda, R.; Kawazoe, H. *Appl. Phys. Lett.* **1997**, *70*, 3561–3563.
- (16) Villora, E. G.; Shimamura, K.; Yoshikawa, Y.; Aoki, K.; Ichinose, N. *J. Cryst. Growth* **2004**, *270*, 420-426.
- (17) Ryu, S.-H.; Kornegay, K. T.; Cooper, J. A.; Melloch, M. R.; *IEEE Trans. on Electron Devices*, **1998**, *45*, 45-53.
- (18) Salahuddin, S.; Datta, S. *Nano Lett.* **2008**, *8*, 405–410.
- (19) Muller, J.; Boscke, T. S.; Schroder, U.; Mueller, S.; Brauhaus, D.; Bottger, U.; Frey, L.;

- Mikolajick, T. *Nano Lett.* **2012**, *12*, 4318–4323.
- (20) Li, K.-S.; Chen, P.-G.; Lai, T.-Y.; Lin, C.-H.; Cheng, C.-C.; Chen, C.-C.; Wei, Y.-J.; Hou, Y.-F.; Liao, M.-H.; Lee, M.-H.; Chen, M.-C.; Sheih, J.-M.; Yeh, W.-K.; Yang, F.-L.; Salahuddin, S.; Hu, C. In *IEEE Intl. Electron Devices Meet.*; 2015; pp 620–623.
- (21) Lee, M. H.; Fan, S.-T.; Tang, C.-H.; Chen, P.-G.; Chou, Y.-C.; Chen, H.-H.; Kuo, J.-Y.; Xie, M.-J.; Liu, S.-N.; Liao, M.-H.; Jong, C.-A.; Li, K.-S.; Chen, M.-C.; Liu, C. W. *IEEE Intl. Electron Devices Meet.*; 2016; pp 306–309.
- (22) Zhou, J.; Han, G.; Li, Q.; Peng, Y.; Lu, X.; Zhang, C.; Zhang, J.; Sun, Q.-Q.; Zhang, D. W.; Hao, Y. In *IEEE Intl. Electron Devices Meet.*; 2016; pp 310–313.
- (23) Si, M.; Su, C.-J.; Jiang, C.; Conrad, N. J.; Zhou, H.; Maize, K. D.; Qiu, G.; Wu, C.-T.; Shakouri, A.; Alam, M. A.; Ye, P. D.; *arXiv:1704.06865*; 2017. *Nature Nanotechnology* in press.
- (24) Li, Y.; Yao, K.; Samudra, G. S.; Effect of Ferroelectric Damping on Dynamic Characteristics of Negative Capacitance Ferroelectric MOSFET. *IEEE Trans. Electron Devices* **2016**, *63*, 3636-3641.

Figure captions

Figure 1 (a) Schematic view of β -Ga₂O₃ NC-FETs. The gate stack includes the heavily n-doped Si as gate electrode, 20 nm HZO as ferroelectric insulator, 3 nm Al₂O₃ as capping layer. 30 nm Ti/60 nm Au are used as source/drain electrodes. 86 nm Sn doped n-type β -Ga₂O₃ is used as channel. (b) Top-view false-color SEM image of representative β -Ga₂O₃ NC-FETs on the same membrane with different channel lengths. (c) Cross-sectional view of HZO/Al₂O₃ gate stack, capturing the polycrystalline HZO and the amorphous Al₂O₃.

Figure 2 (a) Polarization versus voltage characteristics for TiN/20 nm HZO/TiN capacitor at different annealing temperature. The P-V shows clear dielectric to ferroelectric transition after annealing. (b) Polarization versus voltage characteristics for 20 nm HZO/3 nm Al₂O₃ stack annealed at 450 °C at different voltage sweep ranges. (c) Landau coefficients extracted from Fig. 2(a) and the corresponding P-V. (4) Energy versus charge based on experimental Landau coefficients in Fig. 3(c). The negative second order derivative (d^2U/dQ^2) indicates the existence of negative capacitance.

Figure 3 (a) I_D - V_{GS} characteristics in log scale of a β -Ga₂O₃ NC-FET. This device has a channel length of 0.5 μ m and channel thickness of 86 nm. SS versus I_D characteristics of the same device in Fig. 3(a) at (b) $V_{DS}=0.1$ V, (c) $V_{DS}=0.5$ V, and (d) $V_{DS}=0.9$ V. SS below 60 mV/dec at room temperature is demonstrated for both forward and reverse gate voltage sweeps.

Figure 4 (a) I_D - V_{GS} characteristics in linear scale of the same β -Ga₂O₃ NC-FET as in Fig. 3. V_T is extracted by linear extrapolation at $V_{DS}=0.1$ V for both forward and reverse sweeps. (a) I_D - V_{DS} characteristics of the same β -Ga₂O₃ NC-FET as in Fig. 3.

Figure 1.

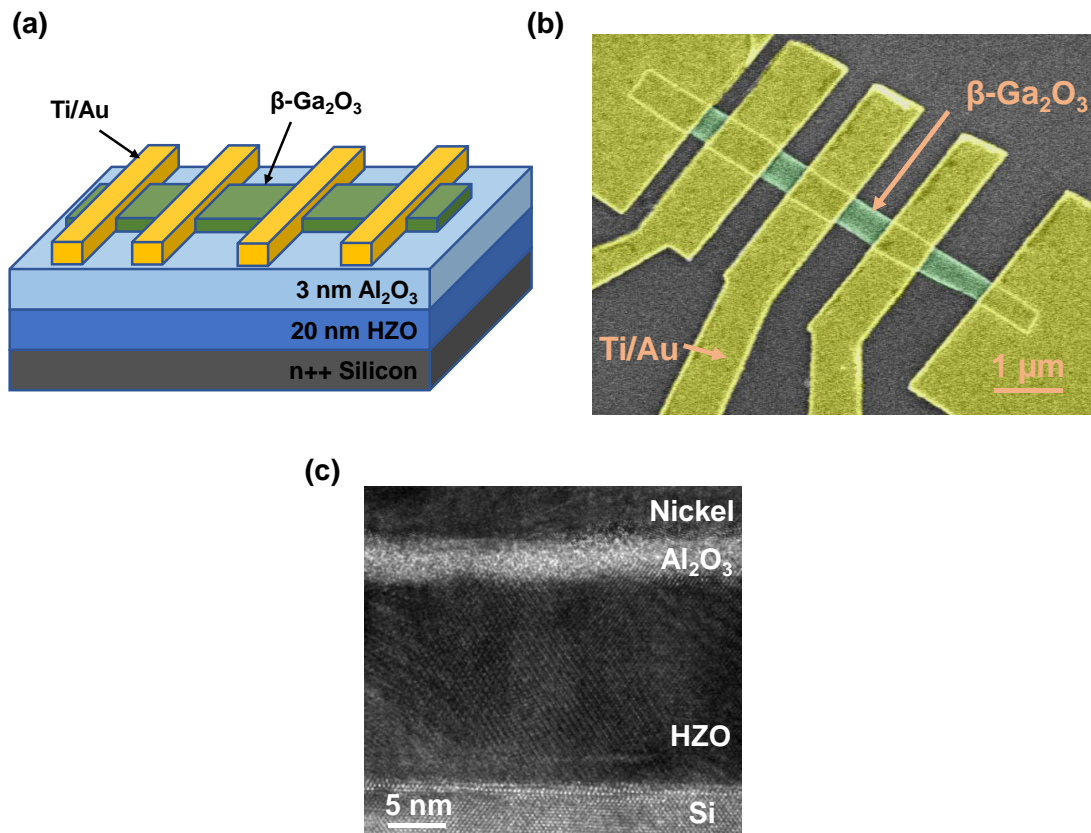


Figure 2.

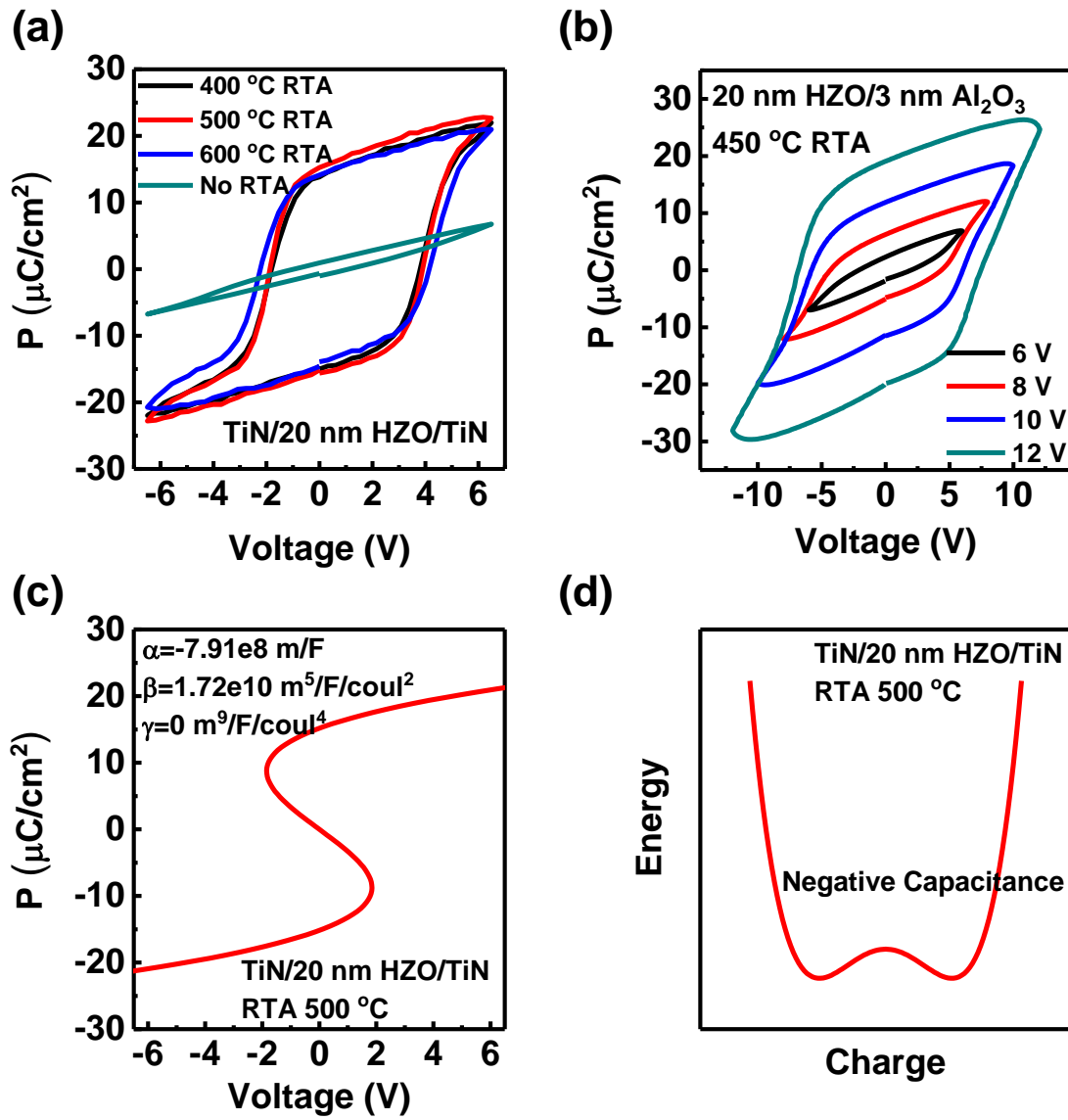


Figure 3.

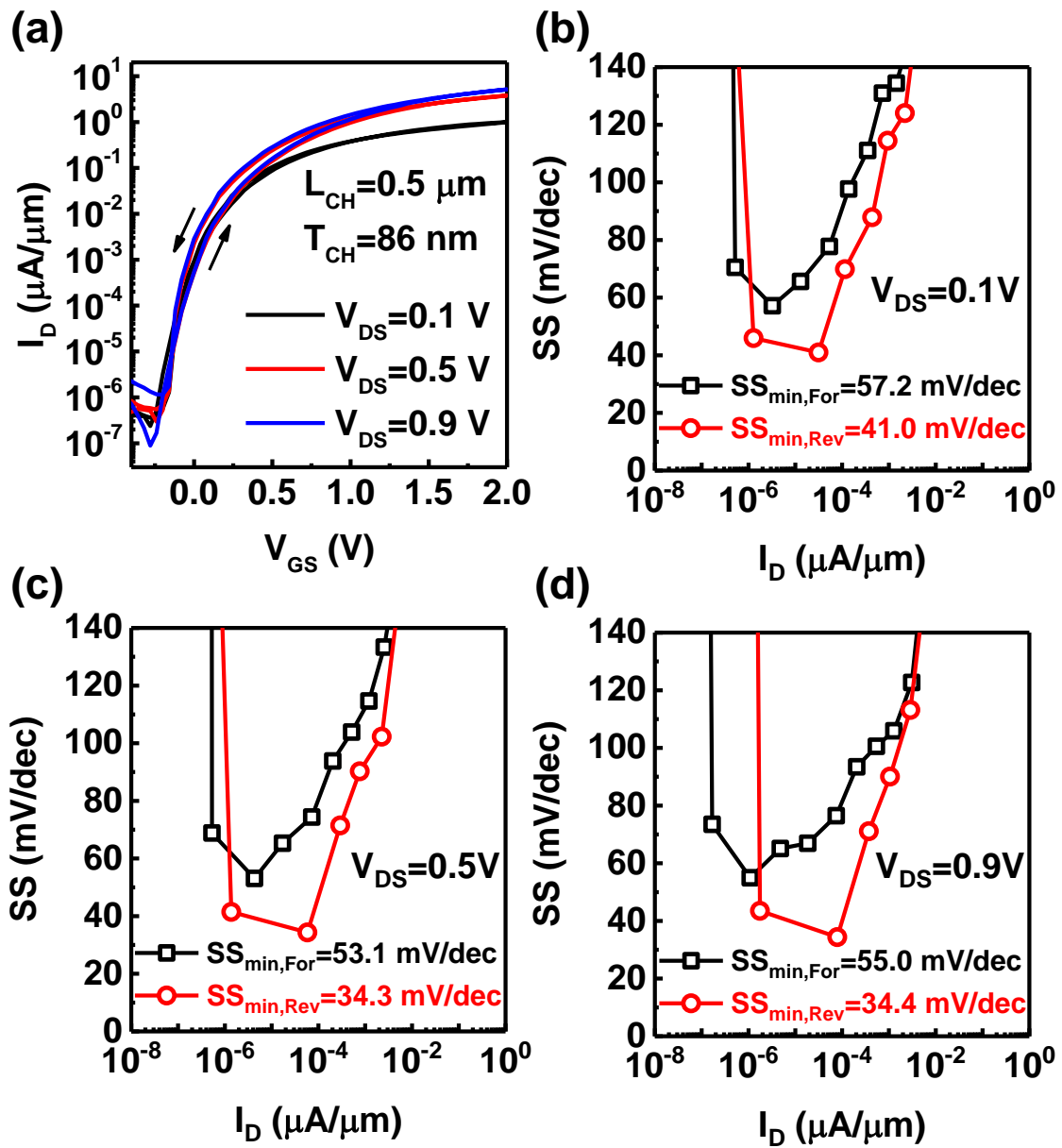
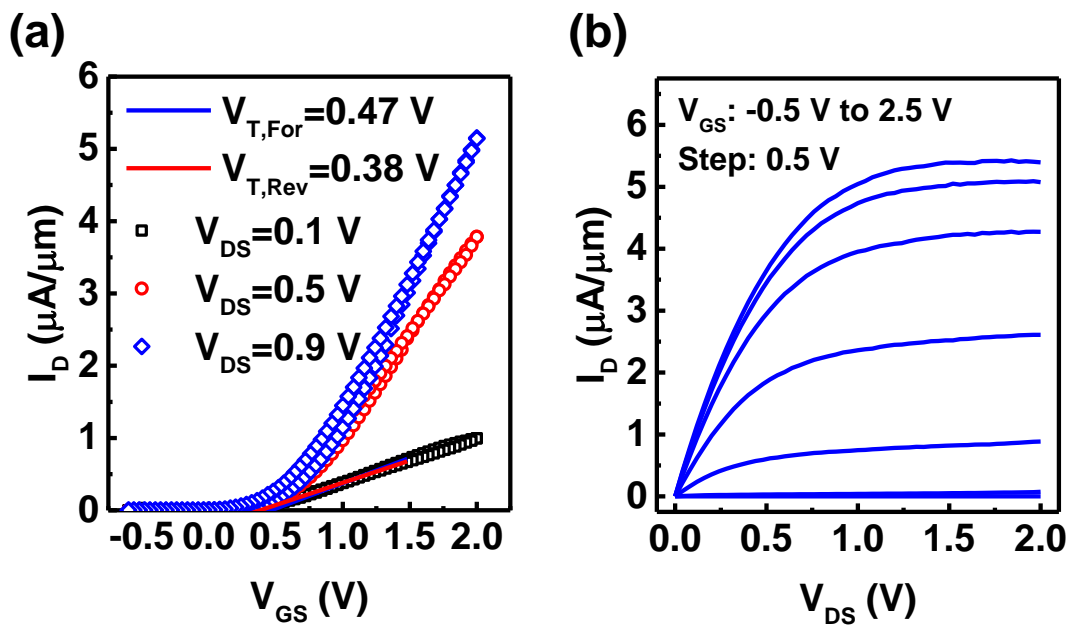


Figure 4.



Supplementary Information for:

β -Ga₂O₃ Nano-membrane Negative Capacitance Field-effect Transistor with Steep Subthreshold Slope for Wide Bandgap Logic Applications

Mengwei Si, Lingming Yang, Hong Zhou, and Peide D. Ye*

School of Electrical and Computer Engineering and Birck Nanotechnology Center, Purdue University, West Lafayette, Indiana 47907, United States

* Address correspondence to: yep@purdue.edu (P.D.Y.)

1. Ga₂O₃ MOSFET with 15 nm Al₂O₃ as gate dielectric

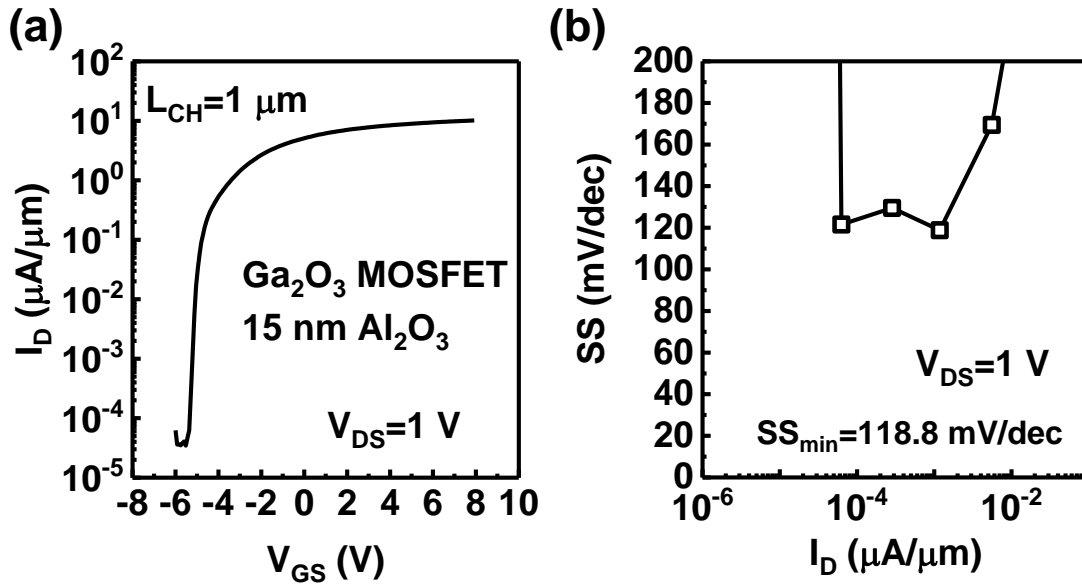


Figure S1. (a) I_D - V_{GS} characteristics in log scale of a β -Ga₂O₃ MOSFET. This device has a channel length of 1 μm . (b) SS versus I_D characteristics of the same device in Fig. S1(a) at $V_{DS}=1 \text{ V}$.

Ga₂O₃ MOSFETs with 15 nm Al₂O₃ only as gate dielectric are fabricated to compare with Ga₂O₃ NC-FETs. Fig. S1(a) shows the I_D - V_{GS} characteristics of a representative Ga₂O₃ MOSFETs measured at $V_{DS}=1 \text{ V}$. Fig. S2(b) shows the SS versus I_D characteristics of the same devices with minimum SS=118.8 mV/dec.